Analyst

Accepted Manuscript

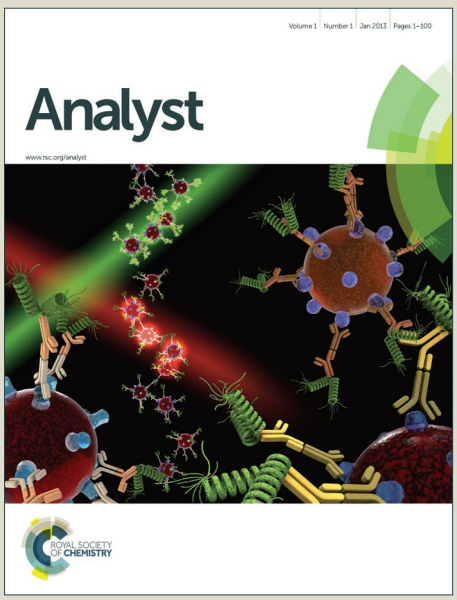

ROYAL SOCIETY OF CHEMISTRY

www.rsc.org/analyst

Desorption of low-volatility compounds induced by dynamic friction between microdroplets and an ultrasonically vibrating blade

D. T. Usmanov,[a,b] K. Hiraoka,[a*] H. Wada,[c] S. Morita,[c] and H. Nonami[d]

[a]Clean Energy Research Center, University of Yamanashi, Takeda-4, Kofu 400-8511, Japan

[b]Institute of Ion-Plasma and Laser Technologies, Dormon Yoli Street 33, Akademgorodok, Tashkent 100125, Uzbekistan

[c]Kyushu Okinawa Agricultural Research Center, National Agriculture and Food Research Organization, 496 Izumi, Chikugo, Fukuoka 833-0041, Japan

[d]Plant Biophysics/Biochemistry Research Laboratory, Faculty of Agriculture, Ehime University, Matsuyama, Japan

Correspondence to : Kenzo Hiraoka; *e-mail:* hiraoka@yamanashi.ac.jp

Abstract

Friction plays an important role in desorption and/or ionization of nonvolatile compounds in mass spectrometry, e.g., sonic spray, easy ambient sonic-spray ionization, solvent-assisted inlet ionization, desorption electrospray, etc. In our previous work, desorption of low molecular weight compounds induced by solid/solid dynamic friction was studied. The objective of this work was to investigate desorption of low-volatility compounds induced by liquid/solid friction. Water/methanol (1/1) micrpodroplets with ~30 μm in diameter were generated by a piezoelectric microdroplet generator. They were injected to analytes deposited on the flat surface of a blade vibrating ultrasonically with the frequency of 40 kHz. Neutral molecules desorbed from the blade were ionized by a helium dielectric barrier discharge (DBD), generating strong signals for samples including drugs, explosives, and insecticides. These signals were not detected when either the blade vibrator or the piezoelectric microdroplet generator was off. In contrast, for ionic compounds such as 1-butyl-3-methylimidazolium bis(trifluoro-methylsulfonyl)imide, p-chlorobenzyl pyridinium chloride, and rhodamine B, strong ion signals were obtained when the vibrator and droplet generator were on, but DBD was off. Sub-nanogram limits of detection were attained for low-volatility compounds.

Keywords: friction, tribology, desorption, microdroplet, ultrasonic vibrator, cavitation

Introduction

Tribology is the study of interactions between surfaces or interfaces in relative motion.[1] In the 1940s, flash temperature was observed at a sliding contact by Boden et al.[2] The tribological phenomena include triboemission of electrons, photons, neutral and charged particles, in addition to heat as the most degraded form of mechanical energy. [3,4]

There are numerous examples in which tribological phenomena were used for desorption/ionization in mass spectrometry. Hirabayashi et al. developed sonic spray ionization (SSI) that uses the friction of a sonic gas flow to nebulize liquid flowing out of a capillary.[5] Eberlin and coworkers further modified SSI as an easy ambient sonic spray ionization mass spectrometry (EASI-MS) that uses the sonic spray for desorption/ionization of solid samples.[6,7] Jarrold et al.[8, 9] studied charge separation in liquid droplets when droplets generated by electrospray, sonic spray, and a vibrating orifice aerosol generator were introduced from atmospheric pressure to vacuum through a capillary. Charge separation was explained by the bag mechanism for droplet breakup and the electrical bilayer at the surface of liquid droplets. In deformed droplets with a bag shape, positive and negative charges are unevenly distributed because of differences in their surface active values.[8] They also found that even negatively charged droplets were formed from positively charged electrospray droplets when they passed through a narrow capillary.[9] Charge separation of droplets inside the capillary was applied to mass spectrometry by McEwen et al.[10] as solvent-assisted inlet ionization (SAII). SAII produces gaseous ions with energy assistance from the pressure drop region and heat, e.g., ionization occurs in the heated inlet tube linking the atmosphere and the first vacuum region of a mass analyzer. Zenobi et al. developed neutral desorption sampling for rapid analysis coupled with extractive electrospray ionization mass spectrometry (EESI-MS).[11,12] They used a neutral gas beam to sample the surface of solid biological objects for in vivo EESI-MS analysis of living matter without sample pretreatment. Desorption of nonvolatile compounds in EESI suggests that the unidirectional gas motion (i.e., localized high pressure) leads to desorption of nonvolatile molecules from the surface. In desorption electrospray ionization (DESI) developed by Cooks et al.,[13] pneumatically-assisted electrospray droplets were directed onto a surface bearing an analyte. The desorbed molecules were efficiently ionized by the impact of the electrospray-charged droplets onto the surface. Dixon et al.[14] and Zhu et al.[15] studied acoustic nebulization of a few μL liquid solutions of biological samples using a quartz ultrasonic transducer. Goodlett and coworkers first applied the surface acoustic wave (SAW) for nebulization of peptide solutions as a microfluidic interface for

MS.[16,17] Trimpin et al. developed an ionization method that uses only the matrix such as 3-nitrobenzonitrile or 2,5-dihydroxyacetophenon.[18] They found that abundant analyte ions including multiple-charge proteins were formed during the sublimation of the matrix under sub-atmospheric pressure. The friction in a matrix accompanied by fracturing (e.g., crack propagation by dislocation) may form charged particles (ejecta).[19] Usmanov et al. developed flash desorption-MS for the analysis of low-volatility compounds using a linearly driven heated metal filament.[20] After touching the sample surface for only 50 ms, the hot filament was moved upward, achieving rapid cooling of the sample. Because of the flash heating/fast cooling, low-volatility compounds are desorbed with minor thermal decomposition. Some contribution from tribodesorption in addition to thermal desorption was suggested for the desorption processes.

In our previous work, desorption of low molecular weight compounds induced by solid/solid dynamic friction was studied.[21] When non-volatile compounds deposited on a perfluoroalkoxy substrate were gently touched by an ultrasonically vibrating blade, efficient desorption of the samples was observed. In the present study, desorption induced by liquid/solid dynamic friction using a piezoelectric microdroplet generator and an ultrasonic blade is described. It was found that the efficiency of desorption induced by liquid/solid friction was about one order of magnitude higher than that by solid/solid friction.[21] Some insight in the high desorption efficiency induced by liquid/solid friction is given.

Experimental

A schematic of the experimental system is shown in Fig.1. An aliquot of 1 μL sample solution of water/methanol (1/1) was deposited on the blade of an ultrasonic cutter (frequency: 40 kHz, oscillation amplitude: ~12 μm, SUW 30-30CT, Suzuki, Japan). The diameter of the deposited sample spot was about 1.5 mm (~2 mm^2). The liquid droplet dried in about 10 min at room temperature.

When the ultrasonic vibrator was turned on with 20 W-power, a slight rise in the blade temperature was observed with time, up to 30 °C within 90 s. All the experiments were performed within 90 s after the blade was cooled down. With 20 W-power applied to the vibrator, the blade did not get wet by the injected droplets. When the vibrating blade was directly immersed into the liquid

solvent (water/methanol), fine mists were generated, i.e., the blade acted as an atomizer.

Microdroplets of water/methanol (1/1) were generated by a piezoelectric microdroplet generator (Microjet, IJHC-10, Shiojiri, Japan) manufactured for ink-jet printers. The droplets of ~30 μm in diameter (volume: ~10 pL) were directed perpendicularly to the flat surface of the blade on which the samples were deposited. The frequency of the droplet generator was set at 100 Hz. The distance between the nozzle of the microjet generator and the blade was set at 1.5 mm. According to the manufacturer's manual, with this travel distance the speed of the microdroplet was ~10 m/s. The distance between the terminal end of the DBD ion source and the blade was 5 mm. The distance between the blade and the MS inlet was 2 mm. The blade bearing an analyte was moved manually across the microdroplet beam with a speed of ~0.5 mm/s by using an *x*-*y*-*z* manipulator.

A fraction of desorbed neutral gas molecules were ionized by using a He DBD ion source developed in our laboratory (ARIOS, Akishima , Japan).[22] The He flow rate was 250 mL/min. In this ion source, the desorbed gas molecules were not exposed to the plasma but were ionized mainly by H_3O^+ and its water clusters $H_3O^+(H_2O)_n$ produced in downstream of the DBD discharge ion source.[22] That is, the present DBD ion source could be regarded as an atmospheric pressure chemical ionization (APCI) ion source.

The explosive compounds of 2,4,6-trinitrotoluene (TNT), 1,3,5-trinitroperhydro-1,3,5- triazine (RDX), and pentaerythritol tetranitrate (PETN) as 1000 ppm solution in acetonitrile were purchased from AccuStandard (New Haven, CT, USA). Morphine and codeine were purchased from Shionogi Pharmaceuticals Ltd. (Osaka, Japan) and cocaine from Takeda Chemical Industries Ltd. (Osaka, Japan). Spinosad, carbaryl, imazalil, gramicidin S and amino acids were purchased from Nissan Chemical Industry Ltd. (Tokyo, Japan). Cholesterol was purchased from Sigma-Aldrich (St. Louis, MO, USA). The thermometer molecule of p-chlorobenzyl pyridinium chloride (p-CBP chloride) was synthesized in our laboratory.[23,24] The ionic liquids of 1-butyl-3-methylimidazolium bis(trifluoro-methylsulfonyl) imide and rhodamine B were purchased from Tokyo Chemical Industry Co. Ltd. (Tokyo, Japan). Methanol (HPLC grade) was purchased from Kanto Chemical Co., Inc. (Tokyo, Japan) and was used without further purification. Pure water was prepared using Simplicity UV (Millipore, Bedford, MA, USA).

The experiments were performed using an Exactive™ Plus Orbitrap MS (Thermo Scientific,

USA). The settings for the Orbitrap were as follows. The temperature of the ion transport tube was 150 °C, the S lens radio frequency (RF) level was 50.0, the S-lens voltage was 25 V, the capillary was grounded, the skimmer voltage was 15 V, and the gate lens voltage was 5.5 V. The maximum ion injection time was 50 ms. The scanning mode for acquisition of the mass spectra was set for a resolution of 35000.

Results

For neutral compounds, analyte ions could be detected only when the ultrasonic vibrator, microdroplet generator, and DBD were all turned on. No analyte ions could be detected when the microdroplet generator and DBD were turned on but the vibrator was off. In the latter case, injected liquid droplets accumulated on the blade to form a liquid pool. Ion signals could also not be detected when the vibrator and microdroplet generator were on but DBD was off. This means that neutral molecules were hardly ionized in the interaction of microdroplets with the vibrating blade. No ions could be detected when the vibrator and DBD were on but the microdroplet generator was off. This means that desorption of analytes from the vibrating blade was negligible. Desorption of neutral analytes took place in the interaction between the microdroplets and the vibrating blade but DBD was necessary to ionize them.

Ionic compounds such as 1-butyl-3-methylimidazolium bis(trifluoro-methylsulfonyl)imide, p-chlorobenzyl pyridinium chloride, and rhodamine B were detected when the vibrator and the microdroplet generator were on but DBD was off. That is, no ionization by DBD was necessary to detect these ionic compounds.

In Table 1, the observed ions for the analytes examined in this work are summarized, along with limit-of-detection (LOD) values. The LOD values shown in Table 1 for morphine, codeine, cocaine, and RDX were found to be more than one order of magnitude lower than those obtained by solid/solid friction.[21]

Supplementary Fig. 1 displays the mass spectra for TNT, RDX, PETN, morphine, codeine, and cocaine. The background ions generated by the DBD ion source were not identified. For TNT, $[TNT]^-$ (*m/z* 227) was observed as the major ion, with $[TNT–H]^-$ (*m/z* 226) and $[TNT–NO]^-$ (*m/z* 197) as minor ions. The ionization mechanisms for TNT were fully discussed in our previous work

using a hollow cathode discharge ion source[25] and an ac corona APCI ion source.[26] For RDX and PETN, the cluster ions of $[M+Cl]^-$, $[M+NO_2]^-$, $[M+NO_3]^-$, and $[M+HCO_4]^-$ (M = RDX and PETN) were observed as major ions. The identification of $[M+HCO_4]^-$ was made by using the high mass-resolution Orbitrap mass spectrometer. The HCO_4^- ion was also observed by direct analysis in real time (DART) [27] and atmospheric pressure corona discharge.[28] In addition to the cluster ions, deprotonated ions $[M–H]^-$ for TNT, RDX, and PETN were observed. In our previous work, $[M–H]^-$ ions were also observed by DBD ionization for TNT, RDX, HMX, and PETN desorbed from liquid droplets by the Leidenfrost effect.[29] The deprotonated ion $[M–H]^-$ is likely to be formed by reaction (1) as suggested for TNT in our previous papers. [25,26]

$$NO_x^- (x=2,3) + M \rightarrow [M–H]^- + HNO_x \qquad (1)$$

The proton affinities of NO_2^-, NO_3^-, and Cl^- are 339.5, 324.3 and 333.4 kcal/mol, respectively.[30] Thus, the contribution of Cl^- to deprotonation reaction (2) is also likely.

$$Cl^- + M \rightarrow [M–H]^- + HCl \qquad (2)$$

The occurrence of reactions (1) and (2) means that the proton affinities of $[M–H]^-$ (M = TNT, RDX, PETN, and HMX) are smaller than those of NO_2^-, NO_3^-, and Cl^-. This is reasonable because the negative charges in $[M–H]^-$ are well delocalized in the negative ions, resulting in their smaller proton affinities.

Morphine, codeine, and cocaine were detected as the protonated form, $[M+H]^+$. Morphine and codeine did not give the dehydrated ion $[M+H–H_2O]^+$ (*m/z* 268). This indicated that these molecules were mildly desorbed/ionized under present experimental conditions. The proton-bound dimer $[2M+H]^+$ at *m/z* 571 was not detected for 100 pg morphine. When the sample amount was increased to 5 ng, the dimer ion appeared with the intensity ratio I {$[2M+H]^+$} / I $[M+H]^+$} of $\sim 3.6\times10^{-3}$. Codeine and cocaine also gave much less abundant dimer ions than monomer ions.

Supplementary Fig. 2(a, b) shows the positive and negative mass spectra for the ionic liquid of 1-butyl-3-methylimidazolium bis(trifluoromethylsulfonyl)imide. In this measurement, He was kept flowing (at 250 mL/min) to transport the generated ions toward the MS inlet, but DBD was off. The cation (C^+) and anion (A^-) as major ions and the cluster ions C_2A^+ and CA_2^- as minor ions were observed. In contrast, no ions could be detected for this compound by solid/solid friction with DBD off.[21]

Figure 2(a) displays the mass spectrum for 100 ng para-chlorobenzyl pyridinium chloride ($M^+\cdots Cl^-$) measured with DBD off. The para-chlorobenzyl pyridinium ion M^+ was observed as the base peak with a much weaker signal of the fragment ion, $[M - \text{pyridine}]^+$. Supplementary Fig. 3 shows the survival yield (SY) $I(M^+)/[I(M^+) + I(F^+)]$ measured as a function of sample amounts deposited on the blade. As shown in the figure, the survival yields (SY>0.9) were nearly independent on the sample amounts. A high SY value indicated that the analyte was mildly desorbed.

Figure 2(b) shows the mass spectrum for 10 ng rhodamine B ($M^+\cdots Cl^-$). A strong ion signal of M^+ at *m/z* 443 was observed with DBD off.

Figure 3 presents the mass spectra of real-world samples. Figure 3(a) shows the mass spectrum of dried apple juice extracted by sticking the blade into an apple. In addition to the ion signals at *m/z* 145, 163, 180, and 198 originating from monosaccharides (Hex), ion signals were observed from disaccharides (Hex_2) at *m/z* 325 and 342. The *m/z* value of the peak appearing at 180 corresponded to the nominal mass of Hex. However, the formation of the molecular ion $Hex^{+\bullet}$ is highly unlikely under ambient ionization.[21] To identify these peaks, we performed a precise mass measurement for the ion at *m/z* 180 using the high mass-resolution Orbitrap mass spectrometer. We found that this ion was not $C_6H_{12}O_6^{+\bullet}$ but $C_6H_{14}O_5N^+$, i.e., $[C_6H_{12}O_6 + H - H_2O + NH_3]^+$. For Hex, reactions (3) and (4) were likely to occur:

$$\text{Hex} + [\text{B+H}]^+ \rightarrow [\text{Hex} + \text{H} - \text{H}_2\text{O}]^+ + \text{H}_2\text{O} + \text{B} \qquad (3)$$

$$[\text{Hex} + \text{H} - \text{H}_2\text{O}]^+ + \text{NH}_3 \rightarrow [\text{Hex} + \text{H} - \text{H}_2\text{O} + \text{NH}_3]^+, \quad (4)$$

where $[B+H]^+$ is the protonating reagent ions produced by DBD. Reaction (3) is the protonation of hexose followed by dehydration. Reaction (4) is the association reaction of $[Hex + H - H_2O]^+$ (*m/z* 163) with ammonia contained in ambient laboratory air. This ion $[Hex + H - H_2O + NH_3]^+$ (*m/z* 180) should have the structure of protonated amino sugar. The association of NH_3 with the carbenium ion $[Hex + H - H_2O]^+$ simply leads to the formation of protonated amino sugar, i.e., a covalent bond is formed by the nucleophilic attack of the lone pair electrons of NH_3 to the vacant p_π orbital of the cationic carbon in the carbenium ion. The ion at *m/z* 198 was assigned as the water cluster of protonated amino sugar. The probability that this ion had the structure, NH_4^+···Hex (*m/z* 198), was low because MS/MS of this ion gave the product ion at *m/z* 180.[21] It was also confirmed that the ion at *m/z* 342 in Fig. 3(a) is not $Hex_2^{+\bullet}$ but $[Hex_2 + H - H_2O + NH_3]^+$. Hogg and Nagabhushan analyzed sugars by chemical ionization using ammonia as a reagent gas.[31] They observed ions at *m/z* 198 and 180 for glucose. The latter ion may have the structure of protonated amino sugar as suggested above.

Figure 3(b) shows the mass spectrum for 10 ng opium. The sample used contained 10 % opium in potato starch. After the sample was dissolved in water/methanol (1/1), the supernatant was used for the measurement. As shown in the figure, the main components of opium such as morphine, codeine, thebaine, paraverine, noscapine, as well as protopine were detected in their protonated forms. Figure 3(c) shows the mass spectrum for the blade after it was used to cut a plastic hose. The plasticizer of bis(2-ethylhexyl)phthalate was detected with high signal intensity. The other peaks were not identified.

The LOD values summarized in Table 1 represent the sample amounts deposited on the blade. Because the finely controlled microdroplet beam was scanned linearly across the sample spot, the sample amounts interrogated for the analysis should be much lower than the deposited amounts. The LOD values listed in Table 1 were nearly the same as those obtained by DESI,[32,33] low temperature plasma ambient ionization[34] and ac-corona APCI[26] for low molecular weight analytes (e.g., TNT, RDX, and PETN) but were much higher than DESI for polar and high molecular weight samples (e.g., arginine and gramicidin S).

Discussion

In this work, the mixed solvent of water/methanol (1/1) was used for the microdroplets. Almost all the samples analyzed in this experiment were dissolvable in this solvent. If the analytes are partly dissolved in the impinging droplet, they might be ionized by the inlet ionization[11] when the progeny droplets containing dissolved analytes pass through the inlet capillary of the mass spectrometer. However, no analyte ions were detected when the DBD ion source was off except for ionic compounds (1-Butyl-3-methylimidazolium bis(trifluoro-methylsulfonyl)imide, p-chlorobenzyl pyridinium chloride and rhodamine B), suggesting that inlet ionization was not a major process in the current method. In addition, monomer ions were observed with much higher abundances than dimer ions. If analytes were transferred to progeny droplets by dissolution, they should be detected as clusters or aggregates after the evaporation of solvent from the progeny droplets. Predominant appearance of monomer ions argues for desorption of analytes in the interaction of microdroplets with the vibrating blade.

It should be noted that the vibrating blade did not get wet by the microdroplets (~10 pL in volume) injected onto the blade surface with 100 Hz. Upon collision of the microdroplets with the blade, the shear stress should act at the interface between the droplet and the blade surface. The shear stress would result in the instant vaporization of the interfacial solvent of the microdroplet. At this moment, desorption of the analytes might occur because of the frictional force acting at the interface, i.e., tribodesorption. The gasification of the interfacial microdroplets is similar to *cavitation*.

In Table 1, the LOD values range from less than 1 pg for cocaine to 10^5 pg for arginine and gramicidin S. There seemed to be some trend that larger size molecules desorbed with more difficulty in the present method. The less efficient desorption might be ascribed to the dissipation of the mechanical friction energy to other processes than desorption of the analytes. The much higher LODs for arginine and gramicidin S (10^5 pg) might be attributed to the stronger adhesion to the metal substrate and/or intermolecular bonds, i.e., energy dispersal as phonons (heat) in solid. In this respect, DESI is much more sensitive for polar and nonvolatile compounds than the present method.

Conclusion

For nonvolatile compounds, desorption prior to ionization is necessary for mass spectrometric analysis. In this study, desorption of low-volatility compounds deposited on the ultrasonic blade was

studied using a piezoelectric microdroplet generator. Upon the collision of microdroplets with the blade vibrating with 40 kHz, desorption of analytes was observed. Cavitation of the microdroplet at the colliding interface may cause desorption of analytes. This rather simple system coupled with the DBD ion source enabled the detection of low-volatility analytes with reasonably high sensitivities. The present method may be applicable to the quick trace analysis of low molecular weight drugs, explosives, insecticides, ionic liquid, etc. but is not suitable for the detection of polar and high molecular weight compounds.

Acknowledgment

The financial supports for this work from the Japan Science and Technology Agency and Grant-in-Aid for Scientific Research (S) are gratefully acknowledged. We thank Prof. L. C. Chen for some help in experiment.

Figure captions

Figure 1. Schematic of the experimental system.

Figure 2. Positive mode mass spectra for (a) 100 ng para-chlorobenzyl pyridinium chloride and (b) 10 ng rhodamine B. The numbers at the upper left hand corner of the plots indicate peak intensities.

Figure 3. (a) Mass spectrum for dried apple juice. (b) Mass spectrum for 10 ng opium. (c) Mass spectrum for the ultrasonic blade after it was used to cut a plastic hose. The numbers at the upper left hand corner of the plots indicate peak intensities.

Supplementary Figure 1. Mass spectra for (a) 1 ng TNT, (b) 10 ng RDX, (c) 10 ng PETN, (d) 100 pg morphine, (e) 100 pg codeine, and (f) 100 pg cocaine. The numbers at the upper left hand corner of the plots indicate peak intensities.

Supplementary Figure 2. Positive (a) and negative (b) mass spectra for ionic liquid, 1-butyl-3-methylimidazolium bis(trifluoromethylsulfonyl)imide. The numbers at the upper left hand corner of the plots indicate peak intensities.

Supplementary Figure 3. Survival yield $I(M^+)/[I(M^+) + I(F^+)]$ measured for para-chlorobenzyl

pyridinium chloride as a function of sample amounts (0.1, 1, 10 and 100 ng) deposited on the blade.

Table 1. Observed ions and LODs in pg for various compounds. The underlined ion represents the major ion. p-CBP^+ stands for the para-chlorobenzyl pyridinium ion.

References

1. J. Y. Park, M. Salmeron, *Chem. Review.,* 2014, **114**, 677.

2. F. P. Boden, M. A. Stone, G. T. Tudor, *Proc. R. Soc. A.* 1947, 188.

3. K. Nakayama, N. Suzuki, H. Hashimoto, *J. Phys. D: Appl. Phys.,* 1992, **25**, 303.

4. K. Nakayama, J-M. Martin, *Wear* , 2006, **261**, 235.

5. A. Hirabayashi, M. Sakairi, H. Koizumi, *Anal. Chem*., 1995, **67**, 2878.

6. R. Haddad, R. Sparrapajn, M. N. Eberlin, *Rapid Commun. Mass Spectrom.*, 2006, **20**, 2901.

7. P. M. Lalli, G. B. Sanvido, J. S. Garcia, R. Haddad, R. G. Cosso, D. R. J. Maia, J. J. Zacca, A. O. Maldaner, M. N. Eberlin, *Analyst*, 2010, **135**, 745.

8. L. W. Zilch, J. T. Maze, J. W. Smith, G. E. Ewing, M. F. Jarrold, *J. Phys. Chem. A,* 2008, **112**, 13352.

9. J. T. Maze, T. C. Jones, M. F. Jarrold, *J. Phys. Chem.,* 2006, **110**, 12607.

10. V. S. Pagnotti, N. D. Chubatyi, C. N. McEwen, *Anal. Chem.*, 2011, **83**, 3981.

11. H. Chen, S. Yang, A. Wortmann, R. Zenobi, *Angew. Chem. Int. Ed.,* 2007, **46**, 7591.

12. H. Chen, A. Wortmann, R. Zenobi, *J. Mass Spectrom.,* 2007, **42**, 1123.

13. Z. Takats, J. M. Wiseman, B. Gologan, R. G. Cooks, *Science,* 2004, **306**, 471.

14. R. B. Dixon, J. S. Sampson, D. C. Muddiman, J. *Am. Soc. Mass Spectrom.,* 2009, **20**, 597.

15. L. Zhu, G. Gamez, H. Chen, K. Chingin, R. Zenobi, *Chem. Commun.,* 2009, 559.

16. S. Heron, R. Wilson, S. A. Shaffer, D. R. Goodlett, J. M. Cooper, *Anal. Chem.,* 2010, **82**, 3985.

17. S. H. Yoon, Y. Huang, J. S. Edgar, Y. S. Ting, S. R. Heron, Y. Kao, Y. Li, C. D. Masselon, R. K. Ernst, D. R. Goodlett, *Anal. Chem.,* 2012, **84**, 6530.

18. S. Chakrabarty, V. S. Pagnotti, E. D. Inutan, S. Trimpin, C. N. McEwen, *J. Amer. Soc. Mass Spectrom.,* 2013, **24**, 1102.

19. R. A. Nevshupa, J. *Friction & Wear,* 2009, **30,** 118.

20. D. T. Usmanov, S. Ninomiya, K. Hiraoka, *J. Am. Soc. Mass Spectrom.,* 2013, **24**, 1727.

21. A. Habib, S. Ninomiya, L. C. Chen, D. T. Usmanov, K. Hiraoka, *J. Am. Soc. Mass Spectrom.,* 2014, **25**, 1177.

22. K. Hiraoka, L. C. Chen, T. Iwama, M. K. Mandal, S. Ninomiya, H. Suzuki, O. Ariyada, H. Furuya, K. Takekawa, *J. Mass Spectrom. Soc. Jpn.,* 2010, **58,** 215.

23. K. Mori, K. Hiraoka, *J. Mass Spectrom. Soc. Jpn.,* 2008, **56**, 33.

24. J. Naban-Maillet, D. Lesage, A. Bossée, Y. Gimbert, J. Sztáray, K. Vékey, J-C Tabet, *J. Mass Spectrom.,* 2005, **40**, 1.

25. A. Habib, L. C. Chen, D. T. Usmanov, Z. Yu, K. Hiraoka, *Rapid Commun. Mass Spectrum.,* 2015, **29**, 601.

26. D. T. Usmanov, L. C. Chen, Z. Yu, S. Yamabe, S. Sakaki, K. Hiraoka, *J. Mass Spectrom*., 2015, **50**, 651.

27. R. B. Cody, J. A. Laramée, H. D. Durst, *Anal. Chem.,* 2005, **77**, 2297.

28. K. Sekimoto, M. Sakai, M. Takayama, *J. Am. Soc. Mass Spectrom.,* 2012, **23**, 1109.

29. S. Saha, M. K. Mandal, L. C. Chen, S. Ninomiya, Y. Shida, K. Hiraoka, *Mass Spectrom.,* 2013, **2**, S008.

30. S. G. Lias, J. E. Bartmess, J. F. Liebman, J. L. Holmes, R. D. Levin, W. G. Mallard, *J. Phys. Chem. Ref. Data,* 1988, Supplement No.1, 1.

[31] A. M. Hoggs, T. L. Nagabhushan, *Tetrahedron Letters,* 1972, **47**, 4827.

32. R. G. Cooks, Z. Ouyang, Z. Takats, J. M. Wiseman, *Science,* 2006, **311**, 1566.

33. Z. Takats, I. Cotte-Rodriguez, N. Talaty, H. Chen, R. G. Cooks, *Chem. Commun.,* 2005, 1950.

34. J. F. Garcia-Reyes, J. D. Harper, G. A. Salazar, N. A. Charipar, Z. Ouyanf, R. G. Cooks, *Anal. Chem.,* 2011, **83**, 1084.

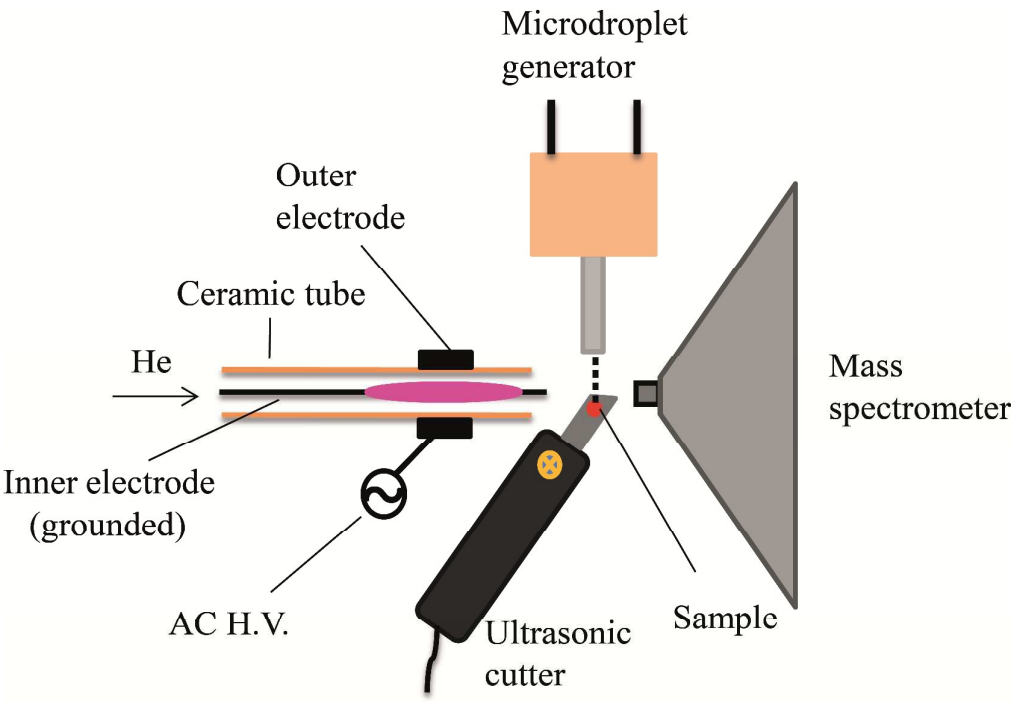

Figure 1. Schematic of the experimental system.

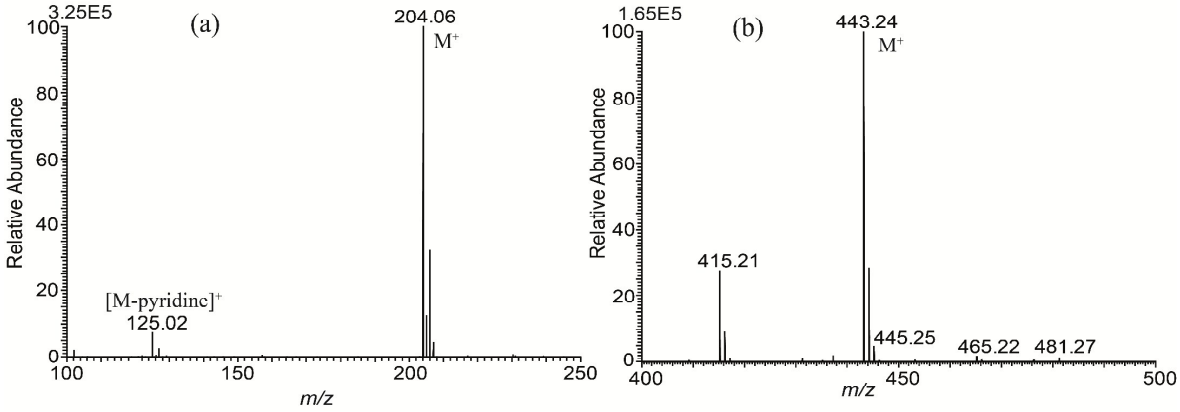

Figure 2. Positive mode mass spectra for (a) 100 ng para-chlorobenzyl pyridinium chloride and (b) 10 ng rhodamine B. The numbers at the upper left hand corner of the plots indicate peak intensities.

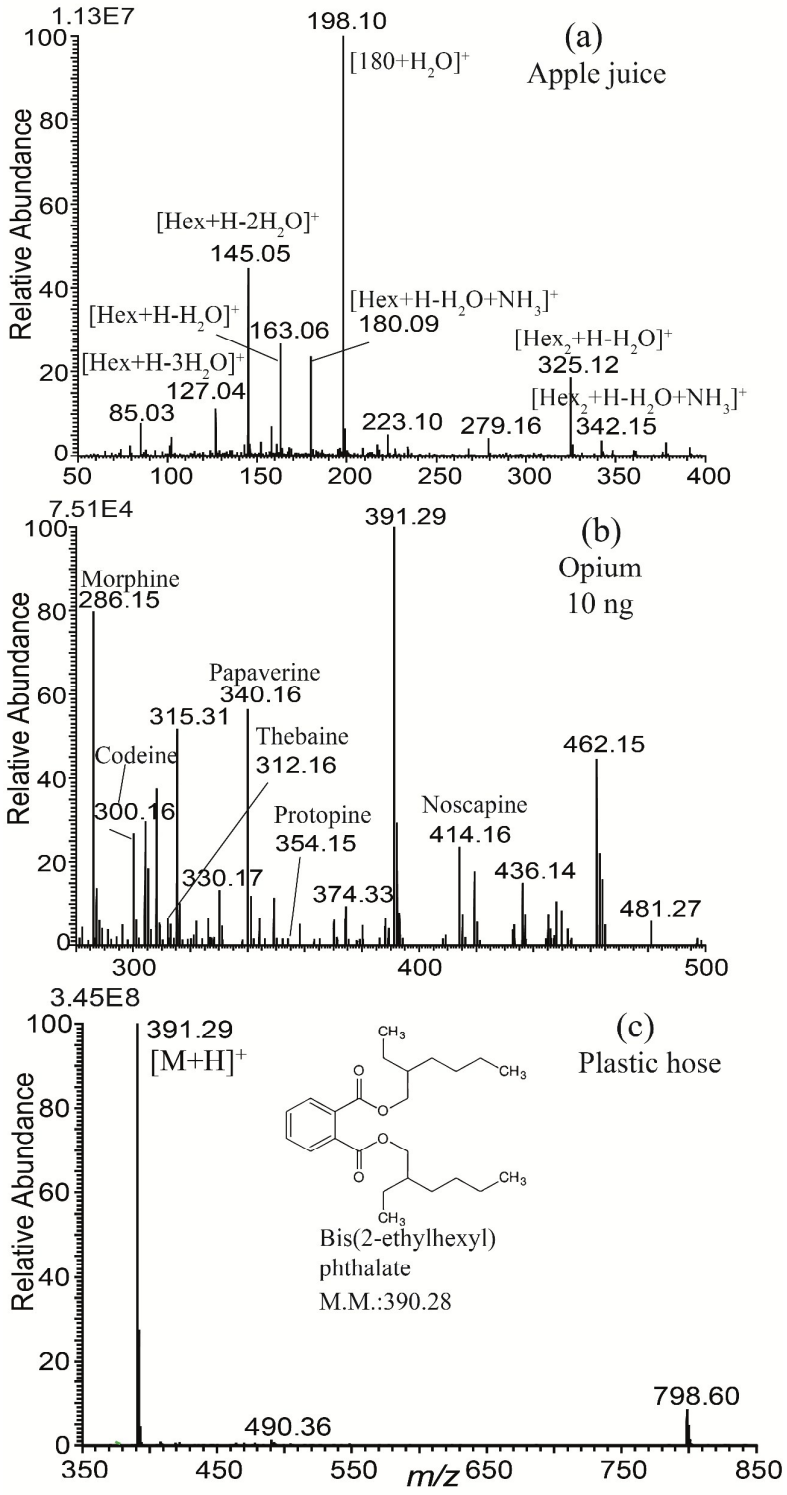

Figure 3. (a) Mass spectrum for dried apple juice. (b) Mass spectrum for 10 ng opium. (c) Mass spectrum for the ultrasonic blade after it was used to cut a plastic hose. The numbers at the upper left hand corner of the plots indicate peak intensities.

Table 1. Observed ions and LODs in pg for various compounds. The underlined ion represents the major ion. p-CBP$^+$ stands for the para-chlorobenzyl pyridinium ion.

Compound	Molecular mass (u)	*m/z*	ion	LOD (pg)
TNT	227	227 226 197	$\underline{M^{-\bullet}}$ $[M-H]^-$ $[M-NO]^-$	10
RDX	222	299 284 267 259 257 221	$[M+HCO_4]^-$ $[M+NO_3]^-$ $[M-H+NO_2]^-$ $[M+^{37}Cl]^-$ $\underline{[M+^{35}Cl]^-}$ $[M-H]^-$	10
PETN	316	393 378 361 352 350 315	$[M+HCO_4]^-$ $[M+NO_3]^-$ $[M-H+NO_2]^-$ $[M+^{37}Cl]^-$ $\underline{[M+^{35}Cl]^-}$ $[M-H]^-$	500
Morphine	285	286	$\underline{[M+H]^+}$	10
Codeine	299	300	$\underline{[M+H]^+}$	1
Cocaine	303	304	$\underline{[M+H]^+}$	0.250
D-arginine	174	175 173	$\underline{[M+H]^+}$ $\underline{[M-H]^-}$	10^5
Gramicidin S	1141	1142	$\underline{[M+H]^+}$	10^5
Carbaryl	201	202	$\underline{[M+H]^+}$	100
Imazalil	296	297	$\underline{[M+H]^+}$	100
Spinosad: Spinosyn A Spinosyn D	731 745	732 746	$\underline{[M+H]^+}$ $\underline{[M+H]^+}$	500
Cholesterol	386	369	$\underline{[M+H-H_2O]^+}$	1000
1-Butyl-3- methylimida-zolium bis(trifluoromethyl-sulfonyl)imide	139 (C^+) 280 (A^-)	139 558 280 699	$\underline{C+}$ C_2A^+	10

			$\underline{A^-}$ CA_2^-	
p-CBP chloride	204 ($p\text{-}CBP^+$)	204 125	$\underline{p\text{-}CBP^+}$ $[p\text{-}CBP\text{–}C_5H_5N]^+$	20
Rhodamine B ($M^+ \cdots Cl^-$)	473 (M^+)	443	$\underline{M^+}$	100